

Remobilization of granitoid rocks through mafic recharge: evidence from basalt-trachyte mingling and hybridization in the Manori–Gorai area, Mumbai, Deccan Traps

Georg F. Zellmer · Hetu C. Sheth · Yoshiyuki Iizuka · Yi-Jen Lai

Received: 9 November 2010 / Accepted: 11 May 2011 / Published online: 14 June 2011
© Springer-Verlag 2011

Abstract Products of contrasting mingled magmas are widespread in volcanoes and intrusions. Subvolcanic trachyte intrusions hosting mafic enclaves crop out in the Manori–Gorai area of Mumbai in the Deccan Traps. The petrogenetic processes that produced these rocks are investigated here with field data, petrography, mineral chemistry, and whole rock major, trace, and Pb isotope chemistry. Local hybridization has occurred and has produced intermediate rocks such as a trachyandesitic dyke. Feldspar crystals have complex textures and an unusually wide range in chemical composition. Crystals from the trachytes cover the alkali feldspar compositional range and include plagioclase crystals with anorthite contents up to

An_{47} . Crystals from the mafic enclaves are dominated by plagioclase An_{72-90} , but contain inclusions of orthoclase and other feldspars covering the entire compositional range sampled in the trachytes. Feldspars from the hybridized trachyandesitic dyke yield mineral compositions of An_{80-86} , An_{47-54} , Ab_{94-99} , Or_{45-60} , and Or_{96-98} , all sampled within individual phenocrysts. We show that these compositional features are consistent with partial melting of granitoid rocks by influx of mafic magmas, followed by magma mixing and hybridization of the partial melts with the mafic melts, which broadly explains the observed bulk rock major and trace element variations. However, heterogeneities in Pb isotopic compositions of trachytes are observed on the scale of individual outcrops, likely reflecting initial variations in the isotopic compositions of the involved source rocks. The combined data point to one or more shallow-level trachytic magma chambers disturbed by multiple injections of trachytic, porphyritic alkali basaltic, and variably hybridized magmas.

Editorial responsibility: M.A. Clynné

Electronic supplementary material The online version of this article (doi:10.1007/s00445-011-0498-4) contains supplementary material, which is available to authorized users.

G. F. Zellmer (✉) · Y. Iizuka
Institute of Earth Sciences,
Academia Sinica, 128 Academia Road, Nankang,
Taipei 11529 Taiwan, Republic of China
e-mail: gzellmer@earth.sinica.edu.tw

G. F. Zellmer
Lamont-Doherty Earth Observatory,
61 Route 9W,
Palisades, NY 10964, USA

H. C. Sheth
Department of Earth Sciences,
Indian Institute of Technology Bombay (IITB),
Powai,
Mumbai 400076, India

Y.-J. Lai
Department of Earth Sciences, University of Bristol,
Wills Memorial Building, Queens Road,
Bristol BS8 1RJ, UK

Keywords Remobilization · Igneous protoliths · Trachytes · Mafic enclaves · Feldspar mineralogy · FE-EPMA mapping · Deccan volcanism

Introduction

Mingling between mafic and silicic magmas is recognized as a fundamental process in active volcanoes and in magma chambers (e.g., Walker and Skelhorn 1966; Yoder 1973; Sparks and Marshall 1986; Snyder 1997). Examples abound worldwide in which mafic (basalt or basaltic andesite) and intermediate to felsic (andesite to rhyolite) magmas have erupted contemporaneously from the same volcanic vent (e.g., Eichelberger et al. 2006). Outcrops also abound where two such contrasting magmas solidified

within a single lava flow, dome, or intrusion, heterogeneous at all scales (e.g., Ishizaki 2007; Zellmer and Turner 2007; Lai et al. 2008). It is because of the differences in their liquidus temperatures, densities, and viscosities that such contrasting magmas do not generally undergo wholesale mixing, so that patches or enclaves of one remain suspended in the other after solidification (e.g., Thomas and Tait 1997; Snyder and Tait 1998). This is magma mingling. However, under suitable conditions, local hybridization along the boundaries of the larger enclaves and wholesale incorporation of the smaller enclaves may occur, resulting in the production of intermediate or hybrid compositions. Such hybridization is magma mixing. Recognizing whether mingling or mixing has occurred is in part dependent on the scale of observation; there are examples of homogeneous-looking rocks at the outcrop or hand specimen scale that are in fact heterogeneous, with mingling of contrasting magmas observable under the microscope (cf. Zellmer and Turner 2007; Humphreys et al. 2009).

Magma mingling and hybridization are significant in that they often indicate mafic recharge of an active felsic magma chamber (Snyder 2000) or partial melting of previously intruded igneous source rocks by reheating, a process that is commonly and hereafter referred to as remobilization (Murphy et al. 2000; Zellmer et al. 2003, 2008, Zellmer 2009). Furthermore, such recharge is often instrumental in bringing about an eruption (Murphy et al. 1998; Snyder 2000), in part due to volatiles exsolved from a newly injected mafic magma, which tend to expel the felsic magma from the chamber. Mingling and mixing of magmas may also be instrumental in the genesis of some intermediate magma compositions (e.g., Yoder 1973; Eichelberger et al. 2006; Reubi and Blundy 2009; Straub et al. 2011).

The ~65 million-year-old Deccan Traps province, India, is one of the world's largest (500,000 km² present-day area) and best-studied continental flood basalt provinces (e.g., Mahoney 1988; Sheth and Melluso 2008). It is dominantly made up of flood lavas of basalt and basaltic andesite, though it also contains rhyolite, trachyte, basanite, nephelinite, and carbonatite magmas (e.g., Lightfoot et al. 1987; Kshirsagar et al. 2011; Sheth et al. 2011). Some spectacular outcrops in the Mumbai area of the Deccan Traps provide insights into the mingling and mixing of mafic (basalt) and felsic (trachyte) magma. Here, with the help of field, petrographic, mineral chemical, and whole-rock geochemical and isotopic data, we discuss the characteristics of these complex mingling and hybridization processes and offer a petrogenetic model for the rock suite.

The Deccan geology of Mumbai

The Deccan lavas were emplaced at ~67–65 Ma, prior to the ~63 Ma separation of the Seychelles from India (Devey

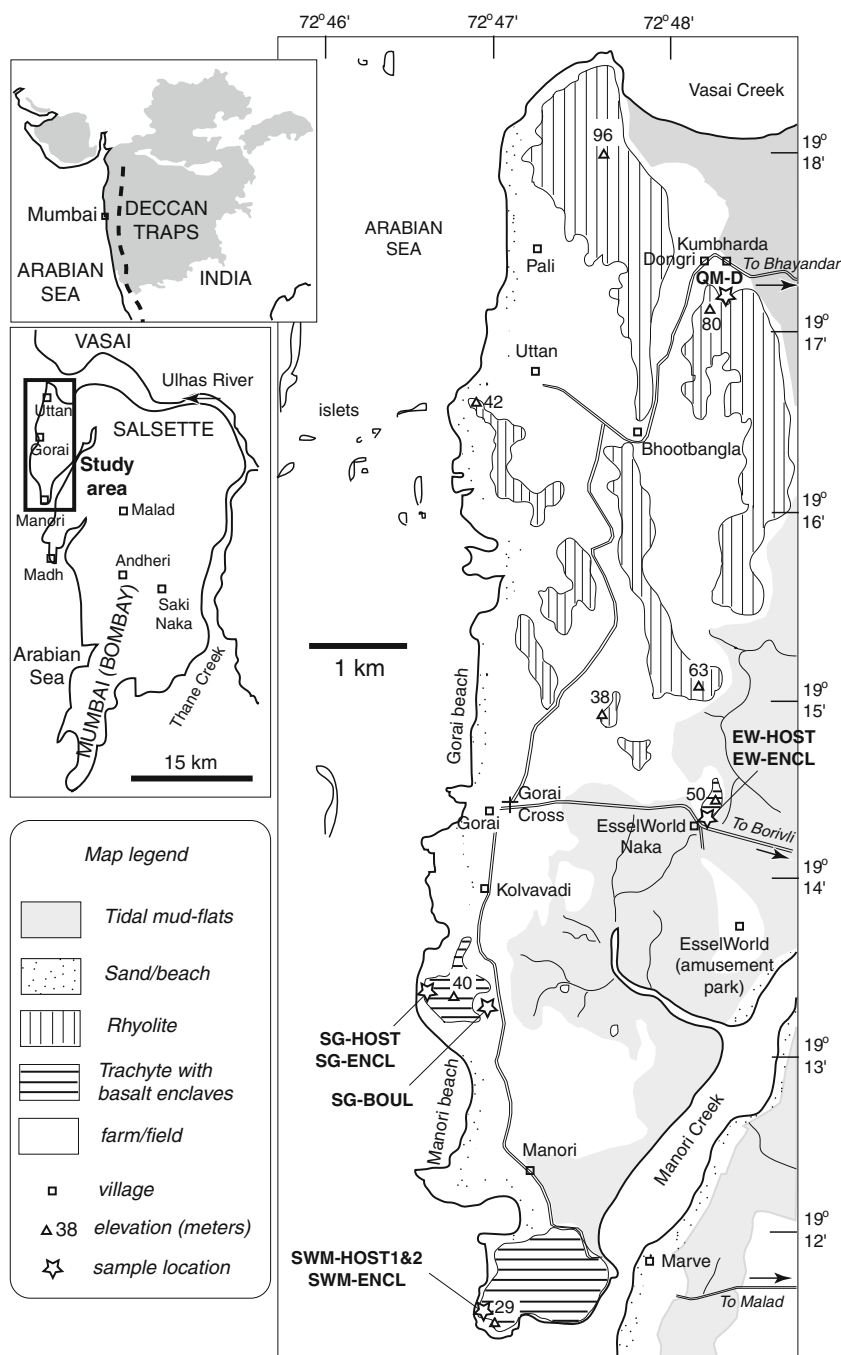
and Stephens 1991). They are at their thickest in the Western Ghats escarpment (>3 km stratigraphic thickness along ~500 km length), parallel to and a few tens of kilometers east of the western Indian coast. The Western Ghats sequence is made up of subalkalic basalt and basaltic andesite lava flows. The geology of the Mumbai area, on the western Indian coast (Fig. 1), is rather unusual in the province: unlike large areas of the Western Ghats and the rest of the province, the Mumbai area includes products of considerable silicic volcanism as well as of mafic subaqueous volcanism (Sethna and Battiwala 1977). In the northern part of Mumbai (Salsette in the older literature), voluminous pyroclastic deposits estimated at >1 km thick (Sethna and Battiwala 1980), and rhyolite flows, constitute the Mumbai Island Formation (Sethna 1999) and are intruded by trachytic units (Lightfoot et al. 1987). In the Manori–Gorai area (Fig. 1), the study area of this paper, these shallow-level trachytic intrusions form good outcrops, though extensive mudflats within the area unfortunately hide all contact relationships between them, so that it is not possible to determine their exact geometry.

Few radioisotopic dates exist for the Mumbai rocks compared to the literature that exists on the Western Ghats sequence (Pande 2002, and references therein). Sheth et al. (2001a, b) obtained ⁴⁰Ar–³⁹Ar ages on trachytes from the Manori and Saki Naka areas of Mumbai (Fig. 1), of 60.4±0.6 and 61.8±0.6 Ma (2σ), respectively. The Gilbert Hill columnar basalt near Andheri, also dated by them, gave an age of 60.5±1.2 Ma (2σ). They observed that these igneous rocks formed during a late phase of Deccan magmatism during the Palaeocene, distinct from the bulk of the 3–5 million years older tholeiitic phase in the province.

Mafic rocks are found as enclaves within the Manori–Gorai trachytes. The enclaves were earlier considered xenoliths by Sethna and Battiwala (1974), who reported major element compositions and petrographic observations. Sethna and Battiwala (1976) subsequently studied outcrops of trachyte profusely invaded by lenses and veins of glassy basalt, at Saki Naka, and recognized the phenomenon as that of contemporaneous intrusion of two magmas. Sethna and Battiwala (1984) then reported a quartz monzonite dyke from Dongri, in the northern part of Mumbai, and by analogy with the Saki Naka outcrops, proposed that the Manori–Gorai trachytes and their mafic enclaves represented contemporaneous magma intrusions. They also suggested that the trachyandesitic dyke was a product of complete hybridization between the two compositionally distinct magmas.

Lightfoot et al. (1987) presented a major and trace element and Nd–Sr–Pb isotopic study of a large sample suite of Mumbai rhyolites and trachytes, and argued that they were generated by partial melting of gabbroic sill complexes in the crust or the deeper parts of the basaltic lava

Fig. 1 Geological map of the study area showing the locations of outcrops studied and samples analyzed. *Inset maps* show the present-day extent of the Deccan Traps (*shaded*) and the Western Ghats escarpment (*heavy broken line*), and the location of the study area within the Deccan province and within Mumbai (too small to be represented to scale on the Deccan Traps *inset map*). Based on Sethna and Battiwala (1974, 1984)



pile, followed by some degree of fractional crystallization. Conversely, Sheth and Ray (2002) proposed an assimilation and fractional crystallization (AFC) model for the trachyte and rhyolite suite, with a basaltic starting magma and a Precambrian granite as a crustal contaminant. Apart from the early work by Sethna and Battiwala (1974), no studies exist of the basaltic enclaves in the Manori–Gorai trachytes. The present contribution fills this gap, with new major and trace element, mineral chemical and Pb isotopic data, and offers several new insights into the development and dynamics of the late-stage Deccan magma plumbing system

and the origin of local hybrid rocks at this classic volcanic rifted margin.

Field geology and samples

Rapid urbanization in Mumbai has destroyed or rendered inaccessible most geological outcrops, including the Saki Naka trachyte that contained extensive basaltic veins (Sethna and Battiwala 1976) and was dated in the ^{40}Ar - ^{39}Ar study of Sheth et al. (2001b). However, mingled basalts and trachytic rocks remain accessible in the Manori–Gorai area.

At Manori, many columnar jointed trachytic units form a rocky coast and are pale brown to buff colored, fine-grained, sparsely phyrific rocks, and generally devoid of vesicles (Fig. 2a). Sethna and Battiwala (1974) have

therefore considered these trachytic rocks to be shallow intrusions into the local tuffs, which, being more erodible, have been removed and form the surrounding extensive tidal flats.

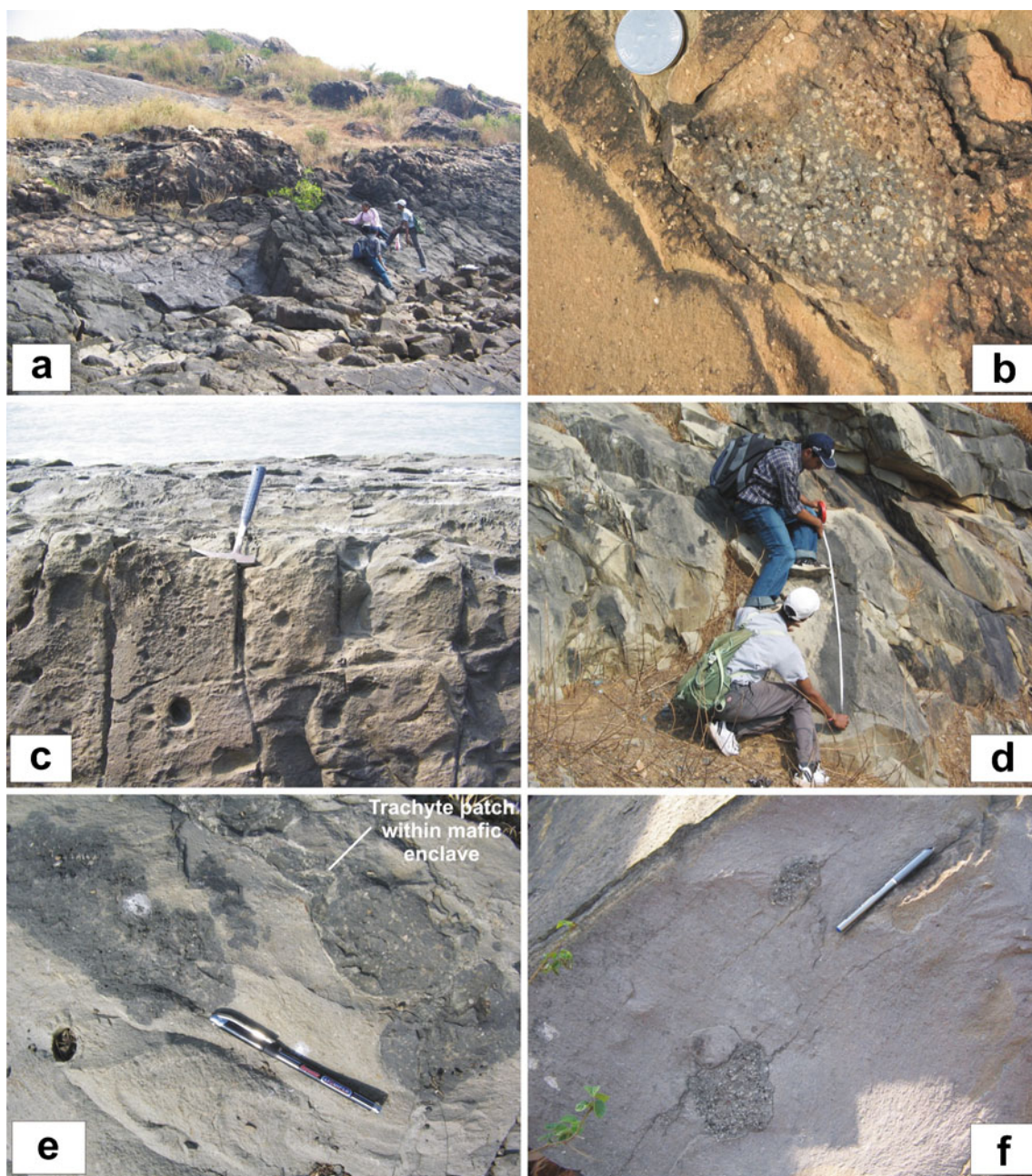


Fig. 2 Field photographs showing basalt-trachyte mingling in the Manori–Gorai area. **a** Columnar-jointed, trachytic unit, dipping westwards (*towards the lower right*) on the Manori coast. **b** A mafic enclave in the Manori trachytic host. Note the highly porphyritic nature of the basalt and the sparse, tiny feldspar phenocrysts in the trachytic unit. Coin for scale is 2 cm. **c** Cavities left in the trachytic unit, Manori coast, by the differential weathering and removal of mafic enclaves. This particular unit dips west, directly away from the viewer, and was dated in the study of Sheth et al. (2001b). **d** Enclave-rich trachytic unit at EsselWorld Naka, with the longest (130 cm)

enclave. Note that not all *dark areas* are enclaves; the trachytic host shows patchy darkening on weathering and alteration, as in the entire right side of the photo. **e** Enclaves of porphyritic basalt in the EsselWorld Naka trachyte, showing *rounded and crenulate shapes*, sharp margins against the trachytic host, as well as a fluidal, *crescent-shaped* trachytic melt patch within one of the mafic enclaves. Note also the cavity at *bottom left* formed by removal of an original mafic enclave. Pen for scale is 15 cm long. **f** Enclaves, again of highly porphyritic basalt, in the trachytic unit south of Gorai village. Note sharp margins against the trachytic host. Pen is 15 cm long

The Manori trachytic rocks contain basaltic enclaves up to tens of centimeters in size (Fig. 2b). Their trachytic hosts contain a few small phenocrysts of white alkali feldspar, visible in outcrop, whereas the basalt enclaves are visibly highly porphyritic, especially with feldspar crystals. The trachytic host rocks show darkening at the margins of many basaltic enclaves. Because of differential erosion in many outcrops, the basaltic enclaves have been removed and cavities left behind (Fig. 2c). Our sample suite from the rocky coast southwest of Manori village contains two trachytic samples taken in close proximity of each other (SWM-HOST1 and SWM-HOST2), as well as a mafic enclave (SWM-ENCL).

Mafic enclaves are most abundant and obvious in the trachytic hillock at EsselWorld Naka, 5 km NE of Manori (Fig. 1). Hundreds of enclaves occur here and range in size from millimeters to tens of centimeters, the longest being 130 cm (Fig. 2d). Many enclaves show crenulate margins with the surrounding trachytic host and local hybridization and darkening. The enclaves are usually porphyritic as at Manori. Interestingly, some of the larger basaltic enclaves contained within the trachytic host themselves contain smaller patches of trachyte (Fig. 2e), although our observations do not resolve if these patches are connected to the host trachyte in the third dimension. Two samples in our suite come from this outcrop (EW-HOST and EW-ENCL).

The trachytic hillock south of Gorai village also shows the mafic enclaves, which are fewer in number and generally small (up to a few centimeters; Fig. 2f). We collected samples (SG-HOST and SG-ENCL) here and also a loose rounded boulder (sample SG-BOUL) of a relatively fresh porphyritic basalt that represents a former enclave, from the eastern slopes of this hillock.

Figure 3 shows field measurements on a total of 114 mafic enclaves from all three localities. The enclaves vary in length from less than 2 mm (below which they become difficult to distinguish from phenocrysts) to 130 cm, and their length distribution follows a negative power law (Fig. 3a). Figure 3b shows the variation of enclave width with length. Whereas there are a few equant enclaves, most enclaves are elongated in shape, with varying length/width ratios of up to ~7.

The remaining sample of this study (QM-D) comes from an abandoned quarry at Kumbharda village, near Dongri, and represents the hybrid trachyandesitic dyke that Sethna and Battiwala (1984) referred to as a “quartz monzonite”. In hand specimen, this is a mesocratic, gray, medium-grained rock with black pyroxene phenocrysts.

Analytical techniques

Elemental distribution maps and quantitative mineral chemical data were obtained with electron probe micro

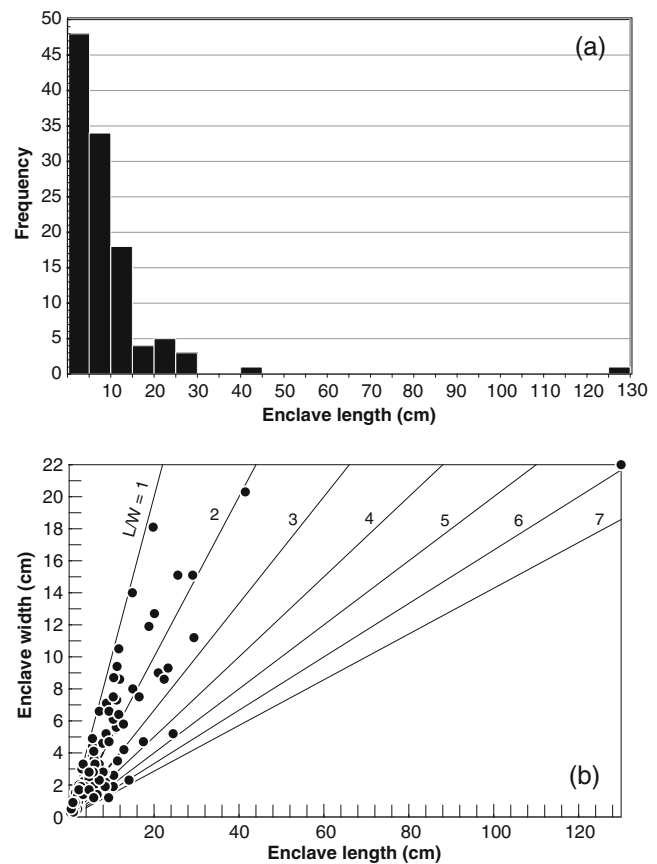


Fig. 3 Field data on 114 mafic enclaves measured in the Manori–Gorai trachytic rocks (only three individuals south of Gorai, 11 southwest of Manori, and 100 at EsselWorld Naka). **a** Frequency histogram for lengths of the enclaves. **b** Plot of enclave width vs. length. *Diagonal lines* are reference lines of constant length/width

analyzers JEOL JXA-8500F and JEOL JXA-8900R, respectively, at the Institute of Earth Sciences, Academia Sinica. Whole rock X-ray fluorescence (XRF) and inductively coupled plasma mass spectrometry analyses were performed at the Department of Geosciences, National Taiwan University. Pb isotope analyses were undertaken at the Department of Earth Sciences, University of Bristol. Details on the analytical methods employed are provided in the [Electronic Supplementary Material](#).

Results

Petrography and mineral chemistry

The petrography of the Manori–Gorai trachytic host rocks and their mafic enclaves has previously been described by Sethna and Battiwala (1974) and pertinent petrographic features are summarized here. Trachytic samples (Fig. 4a) contain phenocrysts of mottled feldspar (0.5 to ~2 mm in size) and sparse crystals of augite and biotite in a fine-

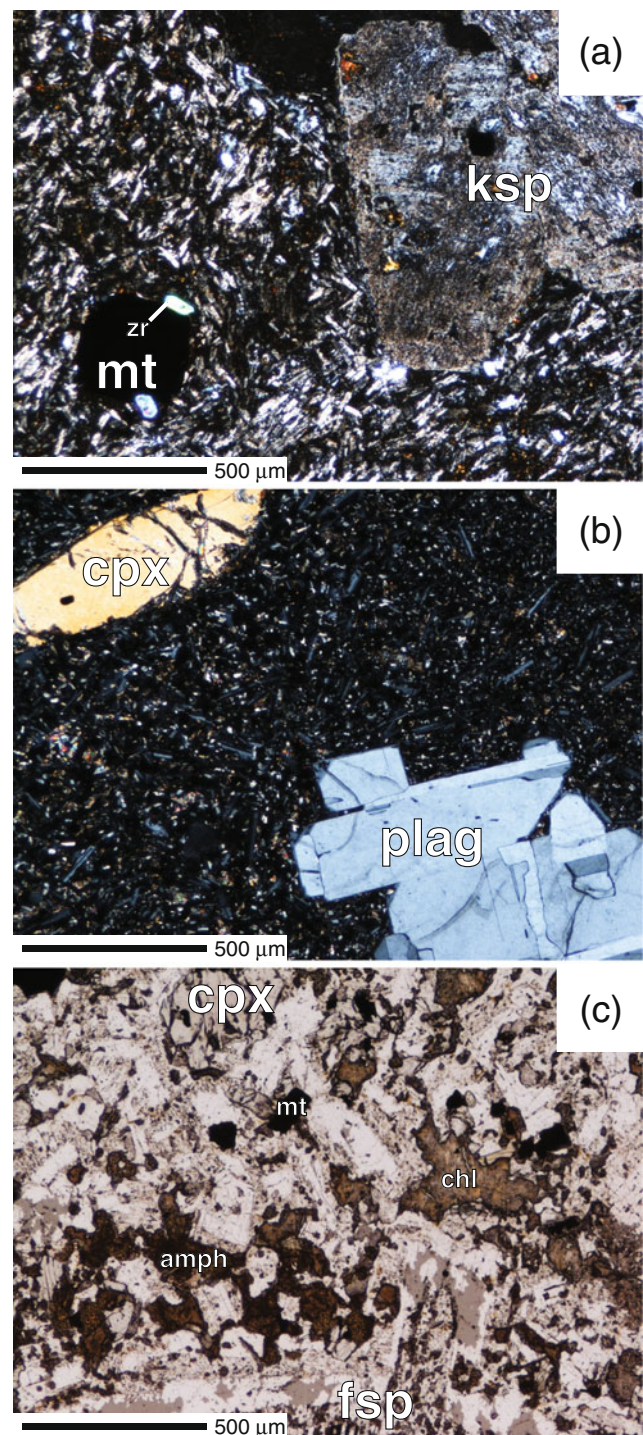
Fig. 4 Photomicrographs of typical samples of the Manori–Gorai rock suite. **a** Trachytic SWM-HOST, crossed polars. Large mottled potassic feldspar (ksp) crystals are set in a fine-grained groundmass dominated by feldspars and some chlorite. Accessory zircon (zr) is closely associated with magnetite (mt). **b** Mafic enclave SG-BOUL, crossed polars. Large plagioclase (plag) crystals, which commonly display twinning, and some pyroxene (cpx) crystals are set in a fine-grained groundmass dominated by plagioclase, pyroxene, oxides, and some chlorite. **c** Dongri trachyandesite QM-D, plane-polarized light. The bottom edge of the image is taken up by part of a large, mottled feldspar crystal (fsp, cf. elemental maps, Fig. 7), with darker spots being artifacts of surface irregularities. Feldspar and pyroxene (cpx) crystals are set in a medium-grained, intergranular groundmass of feldspar, magnetite (mt), and amphibole (amph), the latter intimately associated with chlorite (chl)

grained feldspathic (0.05–0.2 mm) groundmass. Accessory quartz is present as tiny grains (0.03–0.1 mm); thus the rocks are quartz trachytes. Other accessory minerals are hair-like needles of apatite, and zircon grains closely associated with magnetite grains. Chlorite is present as an alteration product, both in the groundmass and in some of the crystals.

Fresh cores of large mafic enclaves (Fig. 4b) are porphyritic, with phenocrysts of unaltered plagioclase (0.2 to >3 mm) and pyroxene (0.5 to ~1 mm), together with sparse altered forsteritic olivine, all set in a glassy to fine-grained groundmass. Some feldspar phenocrysts contain inclusions of zircon. The groundmass of the fresh cores of the mafic enclaves is composed of laths of plagioclase (0.01–0.13 mm) that enclose grains of pyroxene (up to ~0.12 mm) and iron oxides, producing an intergranular texture. Apatite forms tiny fibers in the groundmass plagioclase and iron oxides are dispersed throughout. The enclaves are variably vesicular to highly vesicular (cf. Fig. 2b), although vesicles are occasionally filled with secondary minerals (e.g., zeolites and calcite).

The trachyandesitic dyke from Dongri (Fig. 4c), petrographically described previously by Sethna and Battiwala (1984), who referred to it as a “quartz monzonite”, is porphyritic, with feldspar and pyroxene (augite) phenocrysts set in a medium-grained, mesocratic groundmass. Pyroxenes are compositionally similar to those in the trachytes and richer in iron than those in the fresh mafic enclaves. Some pyroxene phenocrysts show reaction rims of pale brown faintly pleochroic amphibole. The groundmass is intergranular with plagioclase laths surrounding pyroxene, sanidine and magnetite grains, and some amphibole and chlorite. Note that although the rock is quartz normative, there is no modal quartz.

Our electron microprobe study of the Manori–Gorai suite has focused on the petrographically complex feldspar crystals (see Table 1 for representative analyses and Table S1 for the full quantitative dataset). Feldspar phenocryst cores within the trachytic rocks, frequently exceeding 1 mm in size, are characterized by compositionally complex



zoning from andesine to oligoclase (An_{17-45}), with anhedral inclusions of anorthoclase that may themselves contain microinclusions of albite (Fig. 5). The cores show evidence of resorption and are overgrown by up to 200 µm of normally zoned anorthoclase feldspar rims, which in places also contain albitic microinclusions and patchy groundmass inclusions. The rims themselves show embayments at the transition to the groundmass, which is dominated by

Table 1 Representative feldspar analyses from the Manori–Gorai suite

Locality Sample Type Analysis No.	Trachytic host rocks						Mafic enclaves						Trachyandesitic dyke							
	EW		EW		EW		SG		EW		EW		EW		Dongri		Dongri		Dongri	
	HOST fsp-81	HOST fsp-38	HOST fsp-51	HOST fsp-69	HOST fsp-49	EW	SG BOUL fsp-5	SG BOUL fsp-146	ENCL fsp-61	ENCL fsp-6	ENCL fsp-8	ENCL fsp-2	QMD fsp-6	QMD fsp-15	QMD fsp-12	QMD fsp-27	QMD fsp-42			
SiO ₂	57.98	62.50	68.98	67.16	66.39	46.90	53.89	62.36	67.97	67.70	64.82	47.62	56.17	69.68	67.08	64.64				
TiO ₂	0.08	0.02	0.00	0.00	0.04	0.03	0.18	0.10	0.01	0.08	0.03	0.07	0.10	0.05	0.05	0.01				
Al ₂ O ₃	26.42	23.33	19.95	18.62	18.78	34.13	28.12	24.10	20.38	18.51	18.48	33.32	27.09	19.58	18.67	18.44				
FeO	0.41	0.18	0.09	0.32	0.00	0.56	0.72	0.75	0.06	0.19	0.13	0.59	0.56	0.02	0.26	0.01				
MnO	0.04	0.00	0.00	0.00	0.00	0.00	0.03	0.04	0.00	0.00	0.01	0.05	0.00	0.00	0.00	0.04				
MgO	0.04	0.00	0.00	0.00	0.00	0.10	0.12	0.05	0.01	0.00	0.00	0.07	0.06	0.00	0.00	0.00				
CaO	8.86	5.09	0.45	0.18	0.00	17.91	12.10	5.22	0.93	0.33	0.00	17.39	10.27	0.33	0.62	0.10				
Na ₂ O	5.89	7.41	10.06	4.97	0.18	1.21	4.18	7.08	10.28	3.69	0.28	1.61	5.22	10.38	5.31	0.30				
K ₂ O	0.59	1.33	0.71	8.51	16.14	0.05	0.47	1.26	0.14	9.90	16.25	0.12	0.37	0.70	7.92	16.09				
Total	100.31	99.86	100.25	99.75	101.52	100.89	99.81	100.94	99.79	100.39	100.00	100.82	99.84	100.74	99.91	99.62				
An	0.44	0.25	0.02	0.01	0.00	0.89	0.60	0.27	0.05	0.02	0.00	0.85	0.51	0.02	0.03	0.00				
Ab	0.53	0.67	0.93	0.47	0.02	0.11	0.37	0.66	0.94	0.36	0.03	0.14	0.47	0.94	0.49	0.03				
Or	0.03	0.08	0.04	0.53	0.98	0.00	0.03	0.08	0.01	0.63	0.97	0.01	0.02	0.04	0.48	0.97				

sanidine microlites, although anorthoclase microphenocrysts and albite and orthoclase microlites also occur.

Feldspar phenocrysts of the porphyritic mafic enclaves reach several millimeters in size and display weak oscillatory zoning with anorthite content ranging from An₇₂ to An₉₀ (Fig. 6), which is not apparent with optical microscopy (cf. Fig. 4c). Within their cores, they contain inclusions of pyroxene and orthoclase. The outer parts of the crystals contain recrystallized melt inclusions that are mineralogically similar to the groundmass. The groundmass is composed of microlites of plagioclase (An_{<70}), but also contains a significant proportion of alkali feldspar microlites ranging in composition from albite to orthoclase.

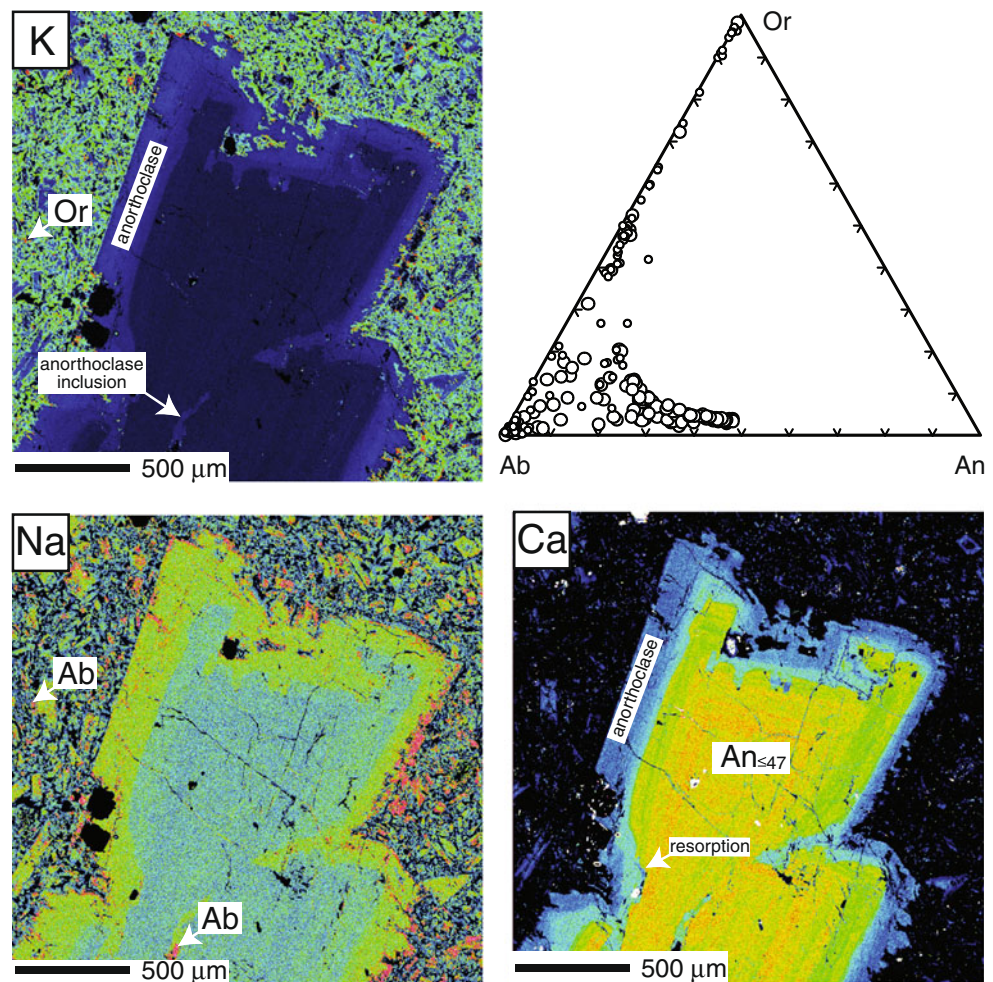
The most complex petrographic features are displayed by the trachyandesitic dyke from Dongri. As evident from Fig. 7, crystal cores are composed of albite with many anhedral inclusions of plagioclase (An_{≤54} and An_{≥80}, with a distinct compositional gap), and some microinclusions of orthoclase. These cores reach >1 mm in size. They are rimmed by up to 200 μm of normally zoned plagioclase (An_{≤54}) to anorthoclase feldspar. In places, this rim extends to large pyroxene crystals that are frequently found within and intergrown with the feldspar crystals. The Dongri dyke is therefore a rare example of a rock that contains the entire natural range of feldspar compositions within individual crystals. The groundmass feldspar is dominated by sanidine (Or₄₅₋₆₀), but also includes microlites of orthoclase, albite, and plagioclase.

Finally, we have also identified carbonate (calcite, siderite, magnesite, and ankerite) and fluorite phases in the studied samples, suggesting that some hydrothermal activity has affected the Manori–Gorai rocks. The morphology and mineral chemistry of these phases will be discussed elsewhere.

Whole rock chemistry

New XRF and loss on ignition (LOI) data of the nine samples analyzed in this study, as well as their normative compositions, are presented in Table 2, and compare well to previously published data from this area (Sethna and Battiwala 1974). LOI values provide insights into the level of alteration suffered by the rocks. They range from 1.58% to 2.78%, with the exception of one sample (SG-ENCL) with a very high value (9.47%) caused by secondary minerals that are common in the Deccan lava flows. We used the SINCLAS program of Verma et al. (2002) to recalculate the major oxide data on an LOI-free basis, compute the normative compositions, and to classify our samples in conformity with International Union of Geological Sciences nomenclature and the total alkali silica (TAS) diagram (Fig. 8, Le Bas et al. 1986). The Middlemost

Fig. 5 Typical feldspar crystal morphology and chemistry of trachytic rocks. This particular example is a crystal from sample SG-HOST, for which K-, Na-, and Ca-elemental maps are presented. *Warmer colors indicate higher concentrations.* In the feldspar ternary, large data points represent analyses from the feldspar crystal, small data points are from groundmass microlites



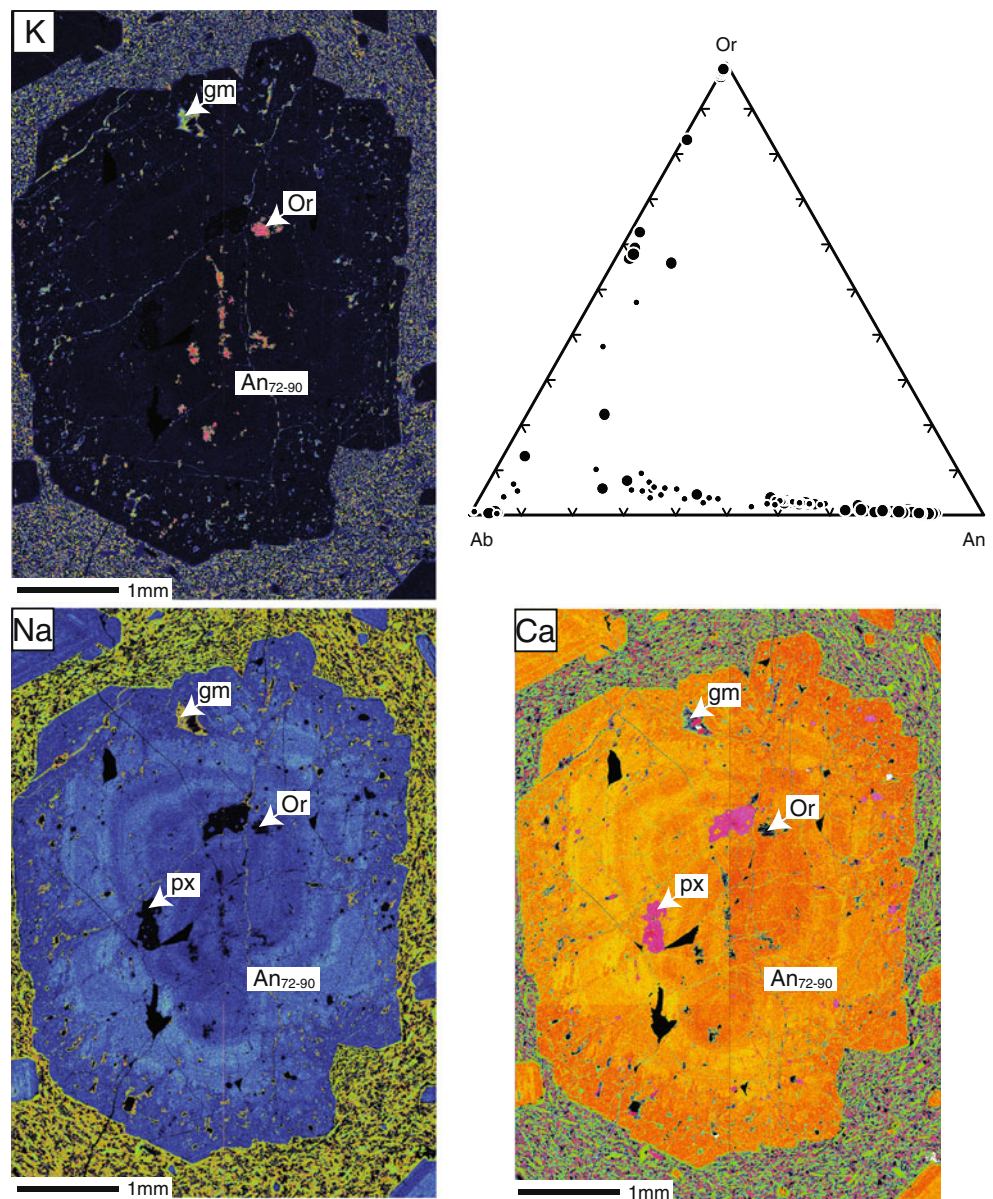
(1989) option provided within SINCLAS was used for dividing the iron into ferrous and ferric iron. The trachytic samples are all quartz normative (8.5% to >13%, cf. Table 2), which is not unexpected noting the accessory modal quartz in these rocks. Intermediate samples (EW-ENCL and QM-D) contain small amounts of normative quartz. Mafic enclaves do not contain normative quartz, and samples SWM-ENCL, SG-ENCL, and SG-BOUL in fact contain normative olivine by 7.5–9%. SG-BOUL also contains 0.6% normative nepheline. We note that Sethna and Battiwala (1974) considered the mafic enclaves to be alkali olivine basalts, pointing out their lower silica and higher alkalis compared to most Deccan basalts and basaltic andesites, which are generally silica-saturated or even oversaturated in normative terms.

The modal differences outlined above are reflected in the TAS diagram, where almost all samples are located above the alkalic/subalkalic divides of Macdonald and Katsura (1964) as well as of Irvine and Baragar (1971), while most of the Deccan flood basalt (and basaltic andesite) lavas, including the Western Ghats lavas, plot below the divides

(Fig. 8). Also shown in Fig. 8 are data for Mumbai “trachytes” and “rhyolites” from Sethna and Battiwala (1980) and Lightfoot et al. (1987). Some of these “trachytes” are dacites or rhyolites, and vice versa. However, the samples of the present study, which were described as trachytes by these former workers, indeed plot in the trachyte field of the TAS diagram.

Trace element data for the Manori–Gorai suite are given in Table 3. The geochemical characteristics of the samples and their internal variation are well displayed by the primitive mantle normalized multi-element patterns. Thus, Fig. 9a shows that all the trachytic rocks of the study are very similar to each other in a wide range of major and particularly trace element contents. All show marked depletions in Ti, P, Sr, and Eu, and enrichments in Pb. Sample Set90 analyzed by Lightfoot et al. (1987) for many of these elements is shown in Fig. 9a, and is closely similar to the trachytic hosts, except notably in its heavy rare earth elements (REE) contents. The latter were measured by instrumental neutron activation, which did not yield accurate results at the low heavy REE (HREE)

Fig. 6 Typical feldspar crystal morphology and chemistry of mafic enclaves. This particular example is a crystal from sample SWM-ENCL, for which K-, Na-, and Ca-elemental maps are presented. *Warmer colors* indicate higher concentrations. In the feldspar ternary, large data points represent analyses from the feldspar crystal, small data points are from groundmass (gm) microlites. Note the presence of alkali feldspar microlites



concentrations of the trachytic rocks (down to less than 1 ppm).

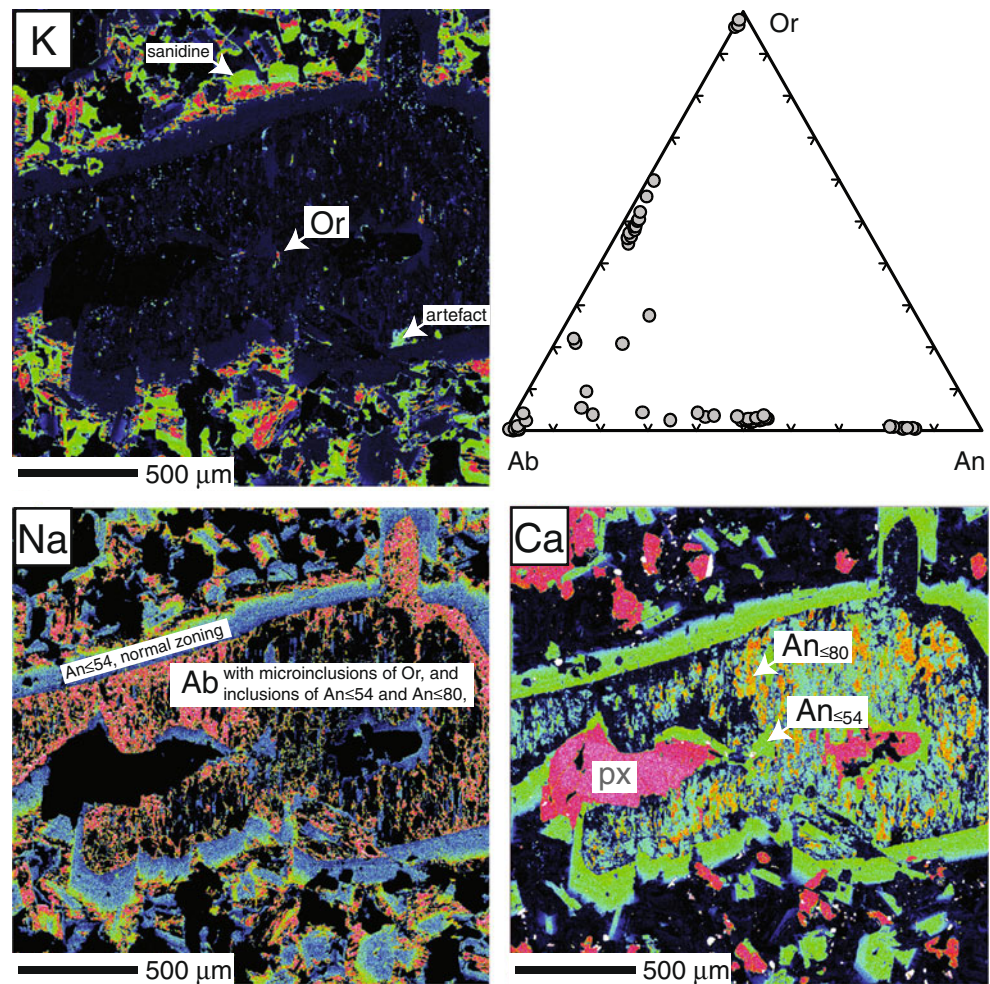
Mafic enclaves SWM-ENCL and SG-BOUL are very similar in most of the elements used in Fig. 9b. Their element patterns are not very smooth but lack the marked anomalies of the trachytic hosts. Notably different from these two enclaves is enclave sample SG-ENCL, which yielded high LOI of >9 wt.%. This sample is significantly enriched in many fluid mobile elements such as U and some large ion lithophile elements (Cs, Rb, Ba, K, Pb), and in Th. Although a variety of processes may lead to compositional variability of mafic enclaves (variable hybridization, autofractionation, late-stage diffusive exchange, e.g., Bacon 1986), the preferential enrichment of fluid mobile elements may be evidence for secondary geochemical alteration. Hence, we refrain

from using results on sample SG-ENCL for petrogenetic interpretations.

Figure 9c compares the intermediate-composition rocks. Sample EW-ENCL, very similar in silica content to the quartz monzonite dyke QM-D, is very close to it in a large range of major and trace elements. The intermediate rock samples also yield depletions in Ti, P, Sr, and Eu, but to a much lesser degree than the trachytic units, and display significant Pb enrichments. A pattern for a “hybrid trachyte” sample Set29, analyzed by Lightfoot et al. (1987), is very close to the above two rocks, except again the HREE, for which INAA data are unreliable.

Finally, the consistency of trace element pattern between similar samples, with the exception of SG-ENCL, indicates that the data can be regarded as reliable

Fig. 7 Typical feldspar crystal morphology and chemistry of the Dongri trachyandesite. This particular example is a crystal from sample QM-D, for which K-, Na-, and Ca-elemental maps are presented. *Warmer colors* indicate higher concentrations. Note that the crystal core does not contain sanidine inclusions; the green K-signals in the core are artifacts of sample surface pits, as verified by comparison to secondary electron images. Data points in the feldspar ternary represent analyses from the feldspar phenocryst and immediately adjacent orthoclase and sanidine microphenocrysts



indicators of petrogenetic processes. Late-stage alteration has modified the geochemistry of SG-ENCL, but apparently did not significantly affect any of the other samples studied here.

Pb isotope data

The Pb isotope data of the Manori–Gorai rocks are tabulated in Table 4 and plotted in Fig. 10. As is the norm in Deccan studies, the Pb isotopic ratios are present-day values. Figure 10a and b show the Pb isotopic compositions of the Manori–Gorai rocks compared to some important stratigraphically defined and geochemically well-characterized formations of the Deccan flood basalts in the Western Ghats region, as well as the previously analyzed samples of the Mumbai rhyolites and trachytes. The Manori–Gorai rocks form a cluster that only partially overlaps with some of the major Deccan flood basalt formations, with $^{206}\text{Pb}/^{204}\text{Pb}$ ranging from 17.089 to 17.540, $^{207}\text{Pb}/^{204}\text{Pb}$ from 15.337 to 15.418, and $^{208}\text{Pb}/^{204}\text{Pb}$ from 37.365 to 38.066.

Discussion

Evidence for hybridization

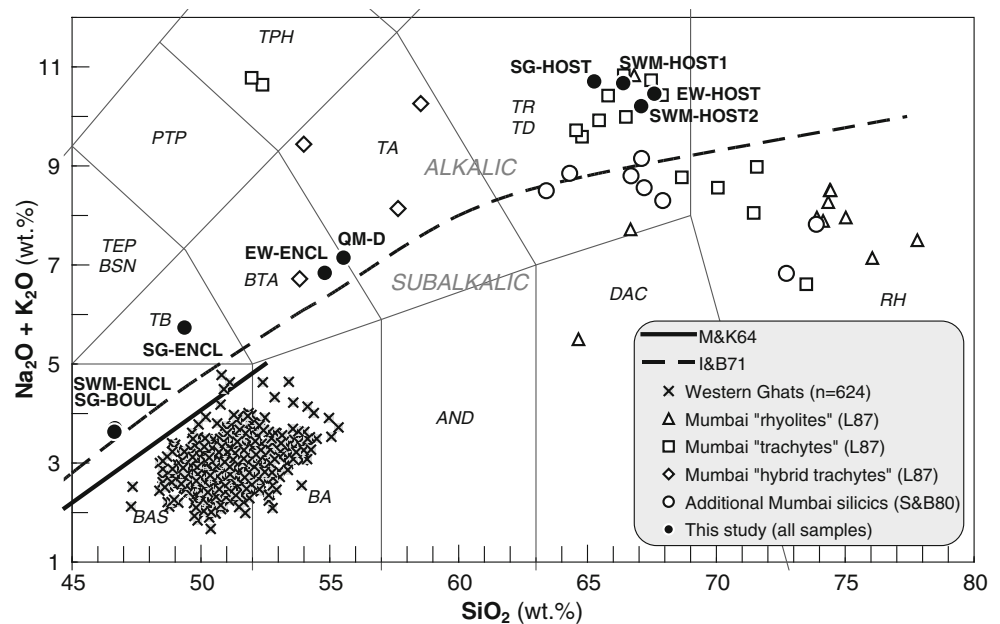
Our new mineral chemical work provides significant evidence for magma hybridization during the petrogenesis of the Manori–Gorai suite, as has been suggested previously (Sethna and Battiwala 1976). In the trachytic rocks (cf. Fig. 5), feldspar crystal cores of andesine ($\text{An}_{\leq 47}$) to oligoclase are strongly resorbed and show anorthoclase overgrowth rims, which themselves show embayments and inclusions of groundmass microlites. The cores may have grown from a compositionally intermediate but inhomogeneous melt. They then underwent resorption, possibly during heating upon magmatic recharge, or due to decompression. Interestingly, the overgrowth rim is not more calcic, but consists of anorthoclase. This is consistent with growth following recharge of a magma with elevated alkali content and suggests that resorption is more likely a result of recharge-related heating than of decompression. An increase in alkali content through recharging magma is

Table 2 Major oxide data (in wt.%) and CIPW norms for the Manori–Gorai suite

Location Rock name Sample	SW of Manori Trachyte SWM-HOST1	SW of Manori Trachyte SWM-HOST2	SW of Manori Subalkalic Basalt SWM-ENCL	S of Gorai Trachyte SG-HOST	S of Gorai Potassic Trachybasalt SG-ENCL	S of Gorai Alkalic Basalt SG-BOUL	EsselWorld Naka Trachyte EW-HOST	EsselWorld Naka Basaltic trachyandesite EW-ENCL	Dongri Trachyandesite QM-D
SiO ₂	65.11	65.87	45.55	63.91	44.67	45.13	66.75	53.07	53.78
TiO ₂	0.54	0.54	3.38	0.63	2.34	3.41	0.53	2.20	2.20
Al ₂ O ₃	16.25	16.34	18.21	16.75	16.99	18.02	16.27	16.13	15.73
Fe ₂ O ₃ ^T	3.75	3.62	10.39	4.02	10.81	10.22	3.03	8.09	8.30
MnO	0.11	0.11	0.15	0.11	0.43	0.15	0.10	0.15	0.15
MgO	1.16	0.75	4.93	0.48	2.55	4.40	0.59	3.47	3.71
CaO	0.84	1.08	11.83	1.70	8.01	12.13	1.27	7.36	6.23
Na ₂ O	5.08	6.35	2.36	5.20	2.92	2.43	4.89	4.45	3.88
K ₂ O	5.39	3.67	1.19	5.29	2.27	1.16	5.44	2.17	3.04
P ₂ O ₅	0.11	0.11	0.56	0.13	0.36	0.56	0.10	0.36	0.44
Total	100.18	100.03	100.57	100.39	100.82	99.83	100.17	100.23	99.92
LOI	1.84	1.58	2.04	2.18	9.47	2.24	1.21	2.78	2.47
Mg#	47.1	37.2	52.6	25.6	37.2	50.1	35.9	52.7	54.6
<i>Q</i>	10.74	10.81	–	8.59	–	–	13.43	0.13	2.26
<i>Or</i>	32.48	22.10	7.19	31.90	14.83	7.07	32.53	13.25	18.55
<i>Ab</i>	43.79	54.71	20.43	44.91	27.30	20.10	41.91	38.91	33.91
<i>An</i>	3.51	4.75	36.46	6.90	29.32	36.04	5.73	18.17	17.05
<i>Ne</i>	–	–	–	–	–	0.60	–	–	–
<i>C</i>	0.81	0.22	–	–	–	–	0.27	–	–
<i>Di</i>	–	–	16.27	0.68	10.01	18.31	–	13.95	9.65
<i>Hy</i>	5.64	4.46	0.45	3.63	0.26	–	3.51	7.52	9.91
<i>Ol</i>	–	–	8.96	–	8.76	7.51	–	–	–
<i>Mt</i>	1.72	1.66	2.35	1.84	3.68	2.34	1.38	2.90	3.29
<i>Il</i>	1.05	1.04	6.57	1.23	4.90	6.69	1.01	4.31	4.32
<i>Ap</i>	0.25	0.25	1.32	0.31	0.93	1.34	0.23	0.85	1.05

Major oxide data were determined by XRF spectrometry. Normative compositions and Mg numbers (Mg#) are as computed using SINCLAS. Fe₂O₃^T is total iron measured as Fe₂O₃. Mg# (Mg Number)=[atomic Mg/(Mg+Fe²⁺)]×100.

Fig. 8 Total alkali-silica diagram (Le Bas et al. 1986), showing the data of the Manori–Gorai suite. Data sources are: this study, Sethna and Battiwala (1980) (SB80), and Lightfoot et al. (1987) (L87). Also shown are 624 samples of the Western Ghats sequence (Beane 1988) for comparison. *Short heavy diagonal line* is the boundary between the alkalic and subalkalic fields, after Macdonald and Katsura (1964). The *curved broken line* is the boundary after Irvine and Baragar (1971). The data are LOI-free values



also consistent with the abundance of sanidine as a groundmass phase.

In the groundmass of the mafic enclaves, Sethna and Battiwala (1974) recognized several irregularly shaped patches composed of albitic plagioclase with a large amount of orthoclase and a little quartz. Texturally, these patches are similar to those observed in the trachytic hosts and it was hence considered possible that they represent the “penetration” of the trachytic magma into the mafic enclaves. Our mineral chemical work (cf. Fig. 6) supports the notion of hybridization of the mafic magma through uptake of alkali feldspar into the basaltic melt during the enclave-forming process; the groundmass of the mafic enclaves contains alkali feldspar microlites ranging in composition from albite to orthoclase.

Whole rock major oxide chemistry led Sethna and Battiwala (1984) to suggest that the 50-m wide trachyandesitic dyke from Dongri, which intrudes local rhyolite lava flows, was a hybrid of ~55% trachytic and ~45% basaltic magmas. The much larger element suite we have acquired appears to corroborate the mixing hypothesis for this rock; Fig. 11a shows that the pattern for the trachyandesitic dyke broadly corresponds to a pattern of a 50:50 bulk mixture of the Manori trachytic host and mafic enclave (SWM-HOST1 and SWM-ENCL). Similarly, the intermediate-composition enclave at EsselWorld Naka, sample EW-ENCL (a basaltic trachyandesite by the TAS diagram), can be modeled as a 50:50 bulk mixture of samples SG-HOST and SG-BOUL (cf. Fig. 11b).

Our data therefore suggest that hybridization between mafic and felsic melts has occurred throughout the Manori–Gorai area of Mumbai. However, while the simple mixing

scenario as portrayed above is broadly consistent for many elements, it cannot be the only process in the genesis of these samples. Notably, the alumina content of the intermediate composition samples is lower than that of any of the trachyte hosts and basaltic enclaves, suggesting that fractionation of feldspar and/or other phases may also have been operating (cf. Sheth and Ray 2002). Depletion of Ti, P, Sr, and Eu in trachytic and intermediate composition samples (Fig. 9) is consistent with magnetite, apatite, and plagioclase as fractionating phases during crystallization. Enrichment in Pb may be a result of hydrothermal alteration of these samples, reflected by the presence of carbonates that are often associated with and may host significant amounts of trace metals, including Pb (e.g., Ionov et al. 1993).

Granitoid remobilization: a possible model for the genesis of the Manori–Gorai suite

The occurrence of orthoclase inclusions within the cores of the bytownite phenocrysts of the mafic enclaves (Fig. 6) points to the existence of orthoclase within the magmatic environment in which the mafic enclaves began to crystallize. Further, the abundant recrystallized melt inclusions within the outer parts of the bytownite phenocrysts suggest rapid crystal growth, and the high alkali content of the groundmass suggests that the mafic melt was richer in potassium than typical for basaltic magmas. These observations may be reconciled by adopting a scenario of influx of hot basaltic melt into cooler granitoid lithologies and the subsequent partial melting of the granitoid rock to form trachytic magma

Table 3 Trace element data (in ppm) for the Manori–Gorai suite

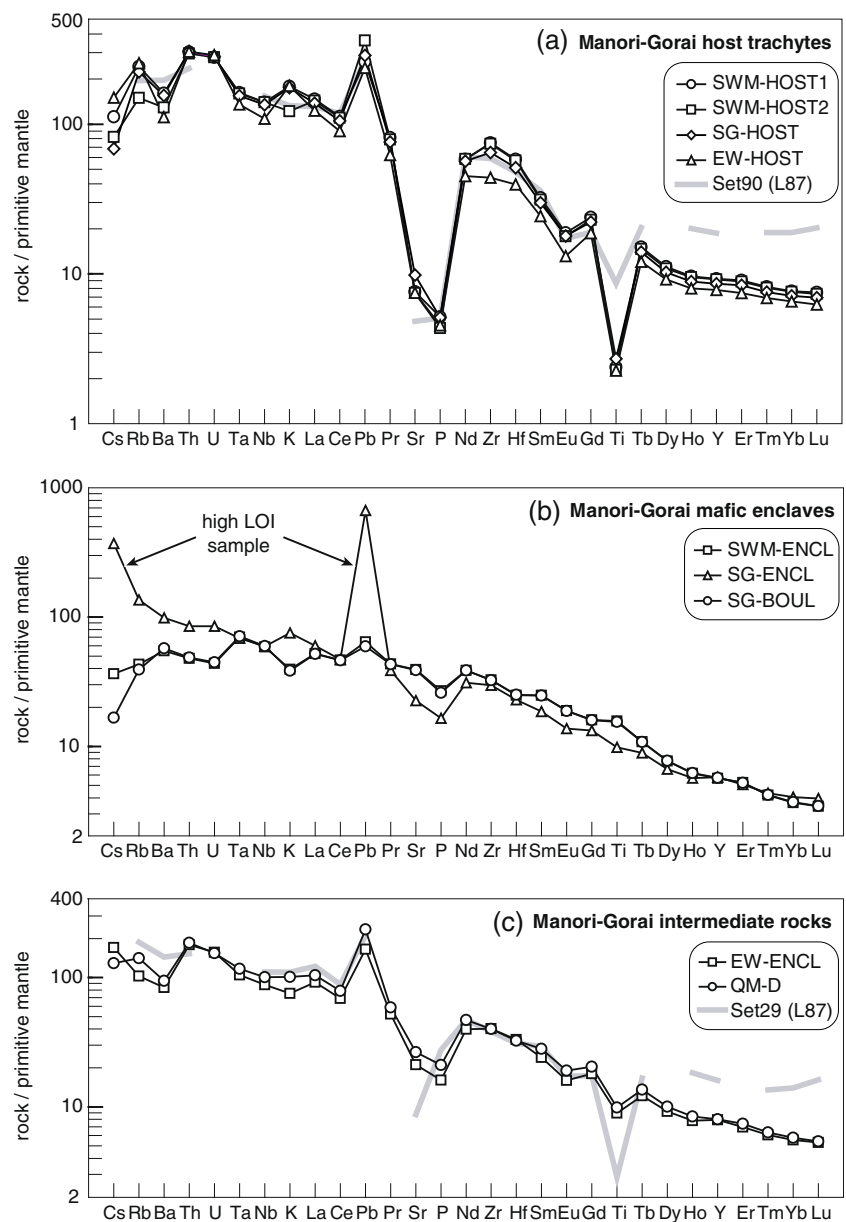
	SWM- HOST1	SWM- HOST2	SWM- ENCL	SG- HOST	SG- ENCL	SG- BOUL	EW- HOST	EW- ENCL	QM-D	QM-D (repeat)	BCR-2 measured	BCR-2 R01 & USGS ^a
Sc	7.26	7.11	25.0	6.90	15.3	24.4	6.26	16.6	15.8	14.7	32.9	33
V	3.30	3.13	285	9.12	179	281	13.0	158	167	157	411	416
Cr	4.60	5.64	58.7	5.53	20.1	48.7	3.54	30.2	58.9	54.7	13.1	18
Co	3.42	3.29	39.9	4.96	23.7	39.2	3.42	23.5	24.5	22.6	36.8	37
Ni	2.72	3.10	55.4	3.51	26.4	52.0	2.57	36.0	40.2	37.5	12.1	
Cu	13.2	13.5	120	16.1	82.1	120	11.9	67.6	41.5	38.5	21.2	19
Zn	79.6	80.3	106.8	68.0	103.3	102	60.0	93.5	101.2	94.2	128.1	127
Ga	26.8	26.5	23.1	26.0	22.2	22.4	23.4	35.3	25.3	24.0	22.4	23
Ge	0.643	0.657	1.46	0.685	1.46	1.37	0.527	1.21	1.25	1.23	1.77	
As	1.76	2.52	1.22	1.57	2.95	1.32	2.02	5.32	1.47	1.34	1.09	
Rb	154	95.2	27.4	142	86.4	24.9	163	65.3	89.5	89.2	48.4	46.9
Sr	161	157	827	207	477	820	158	446	559	553	340	340
Y	42.3	41.9	25.7	39.1	26.3	26.0	35.5	36.2	36.5	36.5	36.6	37
Zr	842	829	366	726	333	364	492	450	448	440	189	188
Nb	100.0	100.0	42.0	96.3	42.4	42.5	77.4	62.9	71.7	71.8	12.1	
Mo	2.35	2.53	1.09	6.06	1.91	1.07	7.28	4.27	4.85	4.82	297	248
Ag	0.226	0.227	0.114	0.212	0.112	0.111	0.142	0.142	0.135	0.137	0.067	
Cd	0.172	0.164	0.096	0.142	0.101	0.097	0.118	0.110	0.113	0.105	0.130	
Sb	0.477	0.567	0.202	0.437	1.10	0.185	0.487	0.880	0.206	0.202	0.355	
Te	0.024	0.024	0.012	0.024	0.012	0.011	0.016	0.016	0.017	0.015	0.005	
Cs	0.883	0.648	0.289	0.540	2.94	0.132	1.19	1.35	1.02	1.04	1.14	1.1
Ba	1122	904	383	1089	690	400	778	586	658	680	678	677
La	101.0	98.8	35.8	95.0	41.3	35.6	84.5	63.2	71.6	69.0	24.7	24.9
Ce	199	196	82.7	187	83.5	82.1	160	123	140	137	52.0	52.9
Pr	22.5	21.8	12.0	21.0	10.7	11.9	17.2	14.4	16.2	16.3	6.87	6.57
Nd	79.0	79.2	52.4	76.6	42.1	52.3	60.8	53.9	63.6	61.6	28.6	28.7
Sm	14.3	13.9	11.0	13.3	8.28	11.0	10.8	10.7	12.5	12.0	6.69	6.57
Eu	3.16	3.00	3.18	3.02	2.31	3.16	2.21	2.70	3.20	3.12	2.13	1.96
Gd	14.2	13.7	9.53	13.2	7.91	9.52	11.2	10.8	12.2	12.0	6.94	6.75
Tb	1.63	1.59	1.17	1.51	0.962	1.17	1.30	1.32	1.47	1.43	1.04	1.07
Dy	8.23	8.02	5.68	7.55	4.91	5.70	6.76	6.79	7.38	7.27	6.41	6.14
Ho	1.58	1.56	1.02	1.46	0.931	1.02	1.31	1.28	1.38	1.35	1.36	1.30
Er	4.34	4.28	2.52	4.03	2.44	2.51	3.58	3.35	3.56	3.51	3.69	3.66
Tm	0.606	0.597	0.310	0.560	0.321	0.312	0.512	0.448	0.469	0.459	0.538	0.564
Yb	3.78	3.75	1.81	3.52	2.00	1.83	3.23	2.74	2.84	2.82	3.42	3.38
Lu	0.556	0.544	0.254	0.514	0.292	0.256	0.463	0.393	0.400	0.398	0.518	0.519
Hf	18.0	17.6	7.69	15.8	7.10	7.77	12.3	10.3	10.0	9.89	4.79	4.8
Ta	6.65	6.56	2.87	6.34	2.81	2.91	5.55	4.30	4.79	4.72	0.88	
W	1.87	2.59	0.330	1.92	7.47	0.372	1.68	2.91	0.924	0.908	0.553	
Tl	0.217	0.208	0.043	0.189	0.110	0.040	0.248	0.117	0.140	0.139	0.276	
Pb	18.5	25.7	4.57	20.4	47.4	4.22	16.9	11.8	16.8	16.9	10.1	11
Th	25.8	25.2	4.07	26.1	7.23	4.13	25.9	15.2	15.8	16.0	5.99	6.2
U	5.88	5.86	0.918	5.92	1.79	0.94	6.09	3.29	3.25	3.31	1.68	1.69

^aData compiled in Raczek et al. (2001) (R01) supplemented with recommended and information values of the US Geological Survey (USGS)

with concomitant rapid crystallization of the mafic melt. Weak oscillatory zoning of the bytownite crystals may be

due to small variations in volatile content within the mafic melts as a result of the competing effects of crystallization

Fig. 9 Primitive mantle-normalized patterns for the Manori–Gorai trachytic units, the mafic enclaves, and the intermediate rocks. Normalizing values are from Sun and McDonough (1989). *Heavy gray patterns* are for samples analyzed by Lightfoot et al. (1987) (L87) that closely match particular samples of this study



and volatile exsolution. The orthoclase crystals included in the bytownite cores may be remnants of the granitoid body, which were taken up into the rapidly growing bytownite crystals at an early stage. The groundmass mineral assemblage points to microscopic-scale mingling between the basaltic and trachytic melt during later stages of crystallization of the mafic enclaves.

The complex feldspar compositional variations of the Dongri dyke (cf. Fig. 7) provide additional insights into the petrogenesis of the suite of samples studied here. Large feldspar cores (formed by an albitic framework hosting calcic plagioclase inclusions) are intergrown with and include large pyroxenes, reminiscent of the phaneritic textures observed in granitoids. The inclusions of anhedral

plagioclase in the feldspar cores are compositionally similar to those found as phenocrysts in the trachytic rocks and texturally appear to fill porosity. Given the bulk geochemical evidence for mixing with basaltic melts, these plagioclase inclusions may have formed from a mixture of a partial melt of granitoid rocks with basalt, which may have acted as the heat source required for partial melting, including partial internal melting of large crystals originally composed of albite. The involvement of basaltic melts in the formation of the plagioclase inclusions is evidenced by some bytownite inclusions (An_{80-86}), which would have been carried by the basaltic melt and would have been preserved within the mixed melt that infiltrated the permeable albitic host crystals.

Table 4 Pb isotopic ratios of the Manori–Gorai suite

Sample	$^{206}\text{Pb}/^{204}\text{Pb}$	$\pm 2\sigma$	$^{207}\text{Pb}/^{204}\text{Pb}$	$\pm 2\sigma$	$^{208}\text{Pb}/^{204}\text{Pb}$	$\pm 2\sigma$
SWM-HOST1	17.3138	0.0006	15.3667	0.0005	37.8689	0.0014
SWM-HOST2	17.0897	0.0006	15.4116	0.0006	37.3653	0.0015
SWM-ENCL	17.4776	0.0007	15.4082	0.0007	37.8217	0.0020
SG-HOST	17.2732	0.0006	15.3620	0.0006	37.8415	0.0016
SG-ENCL	17.1414	0.0007	15.3375	0.0006	37.6640	0.0017
SG-BOUL	17.5028	0.0007	15.3960	0.0007	37.8621	0.0020
EW-HOST	17.4253	0.0008	15.4034	0.0007	37.8791	0.0018
EW-ENCL	17.5399	0.0007	15.3816	0.0007	38.0658	0.0019
QM-D	17.2374	0.0006	15.4174	0.0006	37.5443	0.0016
BCR2 measured	18.7644	0.0007	15.6291	0.0006	38.7510	0.0017
BCR2 USGS ^a	18.750	0.022	15.615	0.006	38.691	0.042

^a Information values of the US Geological Survey (USGS)

Melt evolution during cooling and crystallization may then have resulted in the formation of the normally zoned rim of plagioclase ($\text{An}_{\leq 54}$) to anorthoclase feldspar (cf. Fig. 7). This rim closed remaining intercrystalline porosity that was generated during partial melting of the granitoid as suggested by growth of the rim up against the pyroxenes. Finally, the abundance of sanidine in the groundmass is evidence for rapid cooling during injection of the Dongri dyke.

While the trachytic units observed in the Manori–Gorai area are somewhat simpler than the Dongri dyke in terms of their petrography and mineral chemistry (cf. Fig. 5), it may be argued on the basis of some intriguing similarities that they too are genetically linked to partial melting of previously existing granitoid bodies. For example, the trachytic plagioclase compositional range extends to calcic andesines, overlapping with that of plagioclase from the Dongri dyke. The trachytic rocks also display a similar compositional cluster of sanidine ($\sim\text{Or}_{50}$). Further, significant temperature variations are recorded by the sodic feldspars in the trachytic samples, which display compositional scatter from $\text{Ab}_{<70}$ to albite (Ab_{100}) at variable potassium contents, and a similar scatter is reproduced by some feldspar compositions from the Dongri dyke. The preservation of sanidine in the groundmass is consistent with rapid cooling of this magma upon injection into its upper crustal reservoir.

It is therefore evident from the new data presented here that the rocks from the Manori–Gorai area of Mumbai record remobilization of one or more granitoid rocks by repeated influx of and mixing with basaltic melts, within a complex plumbing system composed of a number of individual magma reservoirs that were fed by periodic influx of variably hybridized magmas. These ranged in composition from trachytic melts generated by partial melting of granitoid rocks, to basalts, which also constitute

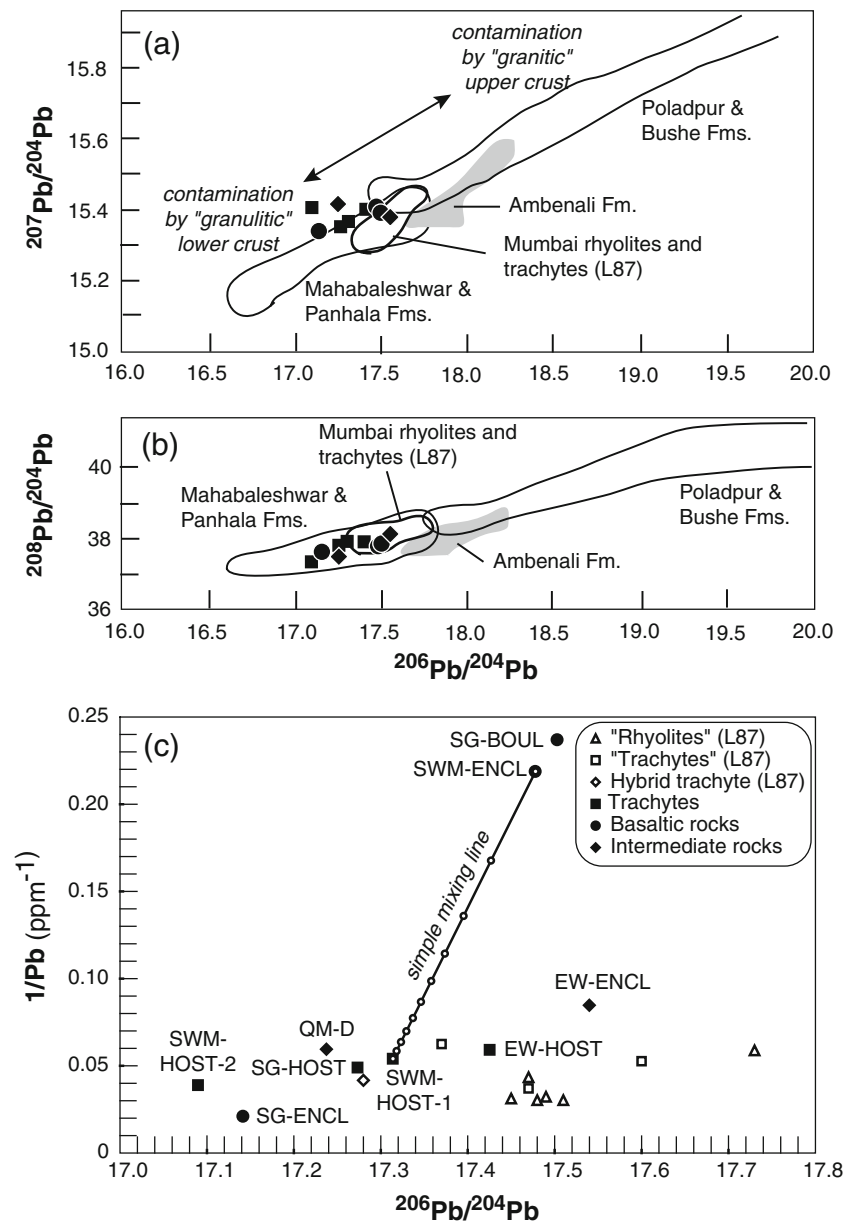
the heat source required for remelting the more evolved rocks. As a result, the feldspar crystals record a history of great temperature and compositional fluctuations ranging from those typical for alkali basaltic magmas down to subsolidus (and subsolvus) conditions of granitoid plutonic rocks.

Preservation of outcrop-scale isotopic heterogeneities

The elevated Pb contents in trachytic and intermediate samples (cf. Fig. 9) may be due to hydrothermal alteration processes, but the degree of enrichment is very similar in all samples, and any effect on Pb isotopic compositions would likely affect all samples in the same way. Further, no correlation is observed between Pb isotopic composition and LOI values. Hence, Pb isotopes may provide insights into the magmatic sources of the Manori–Gorai suite. Figure 10 shows that there is no systematic variation in the Pb isotopic ratios of the Manori–Gorai rocks with their major oxide composition (trachytic, basaltic, or intermediate). Instead, there are distinct isotopic differences between different trachyte host samples even at the outcrop scale (cf. SWM-HOST1 and SWM-HOST2). Some differences in major oxide and trace element abundances of these samples are also observed (cf. Tables 2 and 3). This points to significant small-scale heterogeneities within the trachytic units.

Thus, Pb isotopic ratios are not suitable for testing the simple binary mixing models that can broadly explain the concentrations of many elements in the intermediate samples (cf. Fig. 11). Nevertheless, the observed heterogeneities still need to be consistent with the processes that operated during the genesis of the mingled and hybridized magmas of the Manori–Gorai suite. We therefore suggest that isotopic heterogeneities reflect the involvement of a number of sources for the trachytic host rocks. It appears

Fig. 10 Pb isotopic variations (present-day values) in the Manori–Gorai rocks of this study, previously analyzed rhyolites and trachytes from this area, and in several stratigraphic formations of the Western Ghats Deccan flood basalts (L87= Lightfoot et al. 1987). The stratigraphic formations define distinct arrays resulting from mixing of flood basalt magmas with various continental lithospheric materials. For example, contamination of the Ambenali magmas by ancient U–Th-rich upper crustal materials would produce the Poladpur–Bushe array, whereas contamination by similarly ancient U–Th-depleted lower crustal materials would produce the Mahabaleshwar–Panhala fields (Mahoney et al. 1982; Lightfoot et al. 1990). Both types of crust are inferred or demonstrated (from xenoliths) to exist beneath various parts of the Deccan (Ray et al. 2008). Note that the Manori–Gorai rocks only partially overlap with some of the Western Ghats formations in (a)



that partial melting of a number of small but compositionally and isotopically distinct source rocks is more likely than melting of a larger, homogeneous pluton.

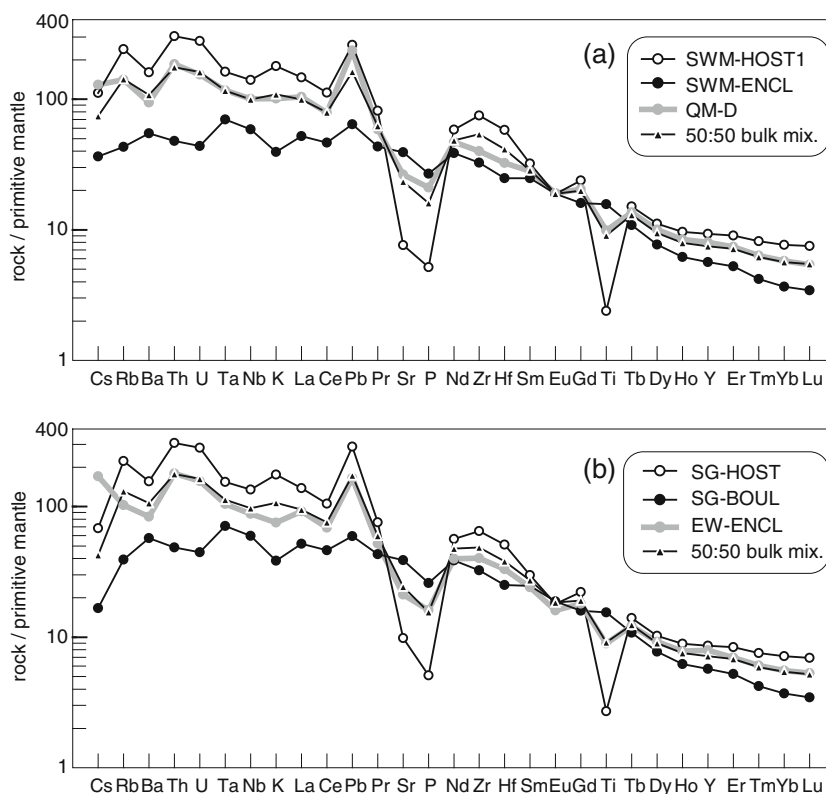
The origin of the inferred granitoid rocks is not further constrained by the data presented here. Their origin could be explained by either near-solidus models, dominantly involving partial melting of deep-seated Deccan basalt lavas or related gabbroic rocks in the lower crust (Lightfoot et al. 1987) or by assimilation of older crustal rocks combined with AFC (cf. Sheth and Ray 2002) to generate the isotopic range displayed by the felsic samples from the area. We note that studies of melt evolution in the lower crust indicate that both partial melting and fractional crystallization may occur at the same time and may thus

not be easily distinguishable by geochemical methods (cf. Annen et al. 2006).

Synthesis: petrogenesis of the Manori–Gorai suite

Based on the data presented here, the principal petrogenetic processes operating in the formation of the Manori–Gorai suite are remobilization of lower to middle crustal granitoids initiated by influx of mafic magmas and hybridization of mafic and felsic magmas. In detail, granitoid rocks at lower to midcrustal levels appear to have been partially melted by influx of mafic magmas from depth, resulting in the formation of trachytic magmas crystallizing in ephemeral chambers (Fig. 12). The recharging mafic magmas

Fig. 11 Primitive mantle normalized patterns (normalizing values from Sun and McDonough 1989) showing bulk mixing models for the hybridized intermediate rocks



experienced cooling and concomitant crystallization (cf. Sparks and Marshall 1986). Hybridization of felsic melt and mafic magmas led to inclusion of some residual orthoclase from the granitoid source into the crystals forming within the mafic enclaves. Trachytic, mafic, and variably hybridized melts of these end-member compositions were channeled upwards through individual dykes (as at Dongri) or conduits of the plumbing system.

We propose that the bulk of the dominantly trachytic melts were ultimately pooled in a shallow magma reservoir, or several such adjacent reservoirs, up to a few kilometers in total lateral extent, under a cover of rhyolite lava flows, tuffs, and pyroclastic rocks. Lack of contact relationships between outcrop localities precludes us from being more specific about the exact geometry of the reservoir. Continued recharge of alkali basalt and basaltic trachyandesite magmas, the latter themselves generated by variable hybridization of alkali basalts with trachytic partial melts, repeatedly disturbed this shallow trachytic reservoir. For example, the hybrid trachyandesitic dyke of Sethna and Battiwala (1984) appears to have formed by remobilization of granitoid rocks due to the influx of basaltic melts, followed by hybridization of granitoid partial melts and the basalts. Cogenetic dykes of similar composition may have intersected the subvolcanic trachytic magma reservoir, as evidenced by the basaltic trachyandesitic enclaves at EsselWorld Naka.

The recharging magmas would intersect the trachytic reservoir(s), and would disintegrate into enclaves of

variable size (cf. Clynne 1999). Disintegration of larger into smaller and yet smaller enclaves is consistent with the negative power law in enclave size distribution (Fig. 3a).

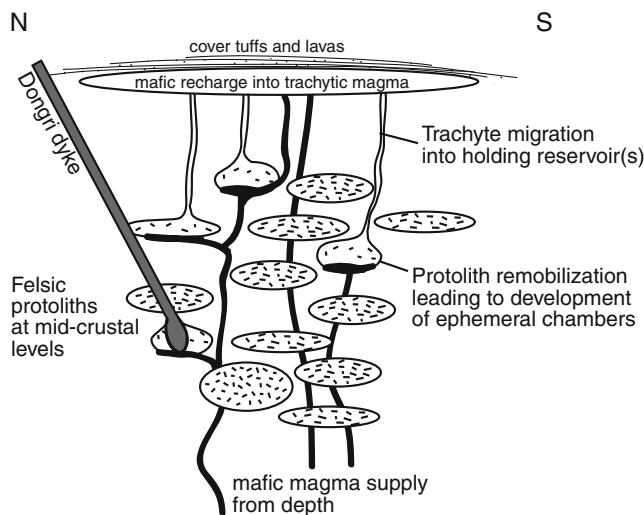


Fig. 12 Crustal magma storage and transfer model for the Manori–Gorai suite, showing remobilization of granitoid rocks (*high-density tick marks*) to form ephemeral magma chambers (*low-density tick marks*), followed by migration of trachytic, mafic and variably hybridized magmas into an upper crustal trachytic reservoir, or several such reservoirs, disturbed by frequent recharge. Some hybrid magmas were channeled upwards through dykes. North (N) and South (S) indicate approximate direction. The vertical scale is not well constrained, as disequilibrium processes preclude meaningful geobarometric work

Enclaves would then have been locally dispersed within the trachytic magma by moderate convection (cf. Snyder 2000), consistent with an abundance of elongated enclaves with length/width ratios of >2 (Fig. 3b) that may indicate shearing of the molten or partially molten enclaves within the trachytic host. Although the distribution of enclaves in host rocks is often heterogeneous (Feeley et al. 2008), it would appear from the great abundance of the basaltic enclaves in the EsselWorld Naka exposure, and their greatly decreased abundance in the outcrops south of Gorai and southwest of Manori, that the time-integrated volume of recharging magmas was highest beneath the EsselWorld Naka area. The differential abundance of mafic enclaves within the Manori–Gorai area, as well as the major oxide, trace element and Pb isotopic heterogeneity of the trachytic hosts on the scale of individual outcrops, suggest that convection was only moderate within the low temperature, shallow reservoir(s). Petrogenesis of the trachytic rocks may have involved a variety of sources (e.g., different crustal contaminants and/or different parental source rocks, cf. Fig. 12).

Concluding remarks

In the Manori–Gorai area of Mumbai, which preserves a record of late-stage Deccan magmatism along the western Indian volcanic rifted margin, alkali basalts occur as mafic enclaves in trachytic hosts. From detailed field, petrographic, mineral chemical, and whole rock chemical and isotopic evidence, we conclude the following:

1. Trachytic hosts and their mafic enclaves were largely liquid when they mingled. The size distribution of the enclaves is consistent with progressive disruptions of larger enclaves into smaller ones. Mineral chemical evidence of partial hybridization of trachytic and basalt magmas, with trachytic material found within some enclaves, is consistent with the field evidence.
2. Feldspar crystals in the trachytic samples show complex zoning patterns, spanning the range from An₄₇ through Ab_{65–99} to Or_{>70}, and provide a record of resorption and overgrowth that results from the mingling of compositionally distinct magmas.
3. Large An_{72–90} feldspar crystals in the mafic enclaves show concentric zoning. Their cores contain orthoclase inclusions, likely derived from granitoid rocks that underwent partial melting; their outer parts are littered with recrystallized melt inclusions, indicating rapid crystal growth. These bytownite crystals have likely grown from the mafic melts when they experienced rapid cooling during injection into their felsic hosts.
4. Feldspar crystals in a hybrid trachyandesitic dyke yield mineral compositions of An_{80–86}, An_{47–54}, Ab_{94–99}, Or_{45–60}, and Or_{96–98}, all sampled within individual crystals. The petrography and mineral chemistry of these crystals is also consistent with partial melting of granitoid rocks through influx of mafic magma, followed by melt mixing, further crystallization, and finally rapid cooling during dyke injection.
5. The whole rock major and trace element chemistry of the samples is broadly consistent with mixing of basaltic and trachytic melts to form the trachyandesitic dyke, and also suggest that some trachytic and intermediate rocks of the area are in fact hybrids themselves. However, outcrop-scale heterogeneity in trachyte Pb isotopic composition suggests multiple sources and inefficient melt homogenization.

The data presented here thus elucidate a complex petrogenetic scenario that involves partial melting of pre-existing granitoid rocks by repeated injection of mafic magmas and hybridization of the granitoid partial melts with the mafic magmas to form melts ranging in composition from quartz trachyte to basaltic trachyandesite. This is evidence for reworking of newly added crustal material in late Deccan times. The outcrops described in this study, representing a complex shallow subvolcanic magma system at a rifted margin, are of significance in understanding the dynamics of source rock remobilization and the mingling and hybridization (mixing) of contrasting magmas. These examples deserve recognition as a spectacular and important rock suite for studying these phenomena and need to be protected in the urban area of Mumbai.

Acknowledgments HCS thanks A. Ghosh, B. Jana, and B. Singh for their field assistance during one of his many visits to these outcrops. We are grateful to C-Y Lee and S-L Chung for access to XRF and ICPMS facilities at National Taiwan University, and to I-J Lin for assistance with the ICPMS analyses. We thank G. Gualda, JG Shellnutt, SF Sethna, S. Viswanathan, and GK Upadhyya for useful discussions and comments on an earlier version of this work. The manuscript benefitted from constructive reviews by S. Seaman and NJ McMillan, and the thorough editorial comments of M. Clynne. This study was partially supported by the National Science Council (96WIA0100363 to GFZ and 97-2116 M001008 to YI) and by Academia Sinica.

References

- Annen C, Blundy JD, Sparks RSJ (2006) The genesis of intermediate and silicic magmas in deep crustal hot zones. *J Petrol* 47:505–539
- Bacon CR (1986) Magmatic inclusions in silicic and intermediate volcanic rocks. *J Geophys Res* 91:6091–6112
- Beane JE (1988) Flow stratigraphy, chemical variation and petrogenesis of Deccan flood basalts from the Western Ghats, India. PhD thesis, Washington State University, USA

- Clynne MA (1999) A complex magma mixing origin for rocks erupted in 1915, Lassen Peak, California. *J Petrol* 40:105–132
- Devey CW, Stephens WE (1991) Tholeiitic dykes in the Seychelles and the original spatial extent of the Deccan. *J Geol Soc* 148:979–983
- Eichelberger JC, Izbekov PE, Browne BL (2006) Bulk chemical trends at arc volcanoes are not liquid lines of descent. *Lithos* 87:135–154
- Feeley TC, Wilson LF, Underwood SJ (2008) Distribution and compositions of magmatic inclusions in the Mount Helen dome, Lassen Volcanic Center, California: insights into magma chamber processes. *Lithos* 106:173–189
- Humphreys MCS, Christopher T, Hards V (2009) Microlite transfer by disaggregation of mafic inclusions following magma mixing at Soufrière Hills volcano, Montserrat. *Contrib Mineral Petrol* 157:609–624
- Ionov DA, Dupuy C, O'Reilly SY, Kopylova MG, Genshaft YS (1993) Carbonated peridotite xenoliths from Spitsbergen: implications for trace element signature of mantle carbonate metasomatism. *Earth Planet Sci Lett* 119:283–297
- Irvine TN, Baragar WRA (1971) A guide to the chemical classification of common rocks. *Can J Earth Sci* 8:523–548
- Ishizaki Y (2007) Dacite-basalt magma interaction at Yakedake volcano, central Japan: petrographic and chemical evidence from the 2300 years B. P. Nakao pyroclastic flow deposit. *J Mineral Petrol Sci* 102:194–210
- Kshirsagar PV, Sheth HC, Shaikh B (2011) Mafic alkalic magmatism in central Kachchh, India: a monogenetic volcanic field in the northwestern Deccan Traps. *Bull Volcanol*. doi:10.1007/s00445-010-0429-9
- Lai Y-M, Song S-R, Iizuka Y (2008) Magma mingling in the Tungho area, coastal range of eastern Taiwan. *J Volc Geotherm Res* 178:608–623
- Le Bas MJ, Le Maitre RW, Streckeisen A, Zanettin P (1986) A chemical classification of volcanic rocks based on the total alkali–silica diagram. *J Petrol* 27:745–750
- Lightfoot PC, Hawkesworth CJ, Sethna SF (1987) Petrogenesis of rhyolites and trachytes from the Deccan Trap: Sr, Nd and Pb isotope and trace element evidence. *Contrib Mineral Petrol* 95:44–54
- Lightfoot PC, Hawkesworth CJ, Devey CW, Rogers NW, van Calsteren PWC (1990) Source and differentiation of Deccan Trap lavas: implications of geochemical and mineral chemical variations. *J Petrol* 31:1165–1200
- Macdonald GA, Katsura T (1964) Chemical composition of Hawaiian lavas. *J Petrol* 5:82–133
- Mahoney JJ (1988) Deccan Traps. In: Macdougall JD (ed) *Continental flood basalts*. Kluwer Academic Publishers, Dordrecht, pp 151–194
- Mahoney JJ, Macdougall JD, Lugmair GW, Murali AV, Sankar Das M, Gopalan K (1982) Origin of the Deccan Trap flows at Mahabaleshwar inferred from Nd and Sr isotopic and chemical evidence. *Earth Planet Sci Lett* 60:47–60
- Middlemost EAK (1989) Iron oxidation ratios, norms and the classification of volcanic rocks. *Chem Geol* 77:19–26
- Murphy MD, Sparks RSJ, Barclay J, Carroll MR, Lejeune A-M, Brewer TS, Macdonald R, Black S, Young S (1998) The role of magma mixing in triggering the current eruption at the Soufrière Hills volcano, Montserrat, West Indies. *Geophys Res Lett* 25:3433–3436
- Murphy MD, Sparks RSJ, Barclay J, Carroll MR, Brewer TS (2000) Remobilization of andesite magma by intrusion of mafic magma at the Soufrière Hills volcano, Montserrat, West Indies. *J Petrol* 41:21–42
- Pande K (2002) Age and duration of the Deccan Traps, India: a review of radiometric and palaeomagnetic constraints. *Proc Ind Acad Sci (Earth and Planet Sci)* 111:115–123
- Raczek I, Stoll B, Hofmann AW, Jochum KP (2001) High-precision trace element data for the USGS reference materials BCR-1, BCR-2, BHVO-1, BHVO-2, AGV-1, AGV-2, DTS-1, DTS-2, GSP-1 and GSP-2 by ID-TIMS and MIC-SSMS. *Geostand Newslett* 25:77–86
- Ray R, Shukla AD, Sheth HC, Ray JS, Duraiswami RA, Vanderkluyzen L, Rautela CS, Mallik J (2008) Highly heterogeneous Precambrian basement under the central Deccan Traps, India: direct evidence from xenoliths in dykes. *Gondwana Res* 13:375–385
- Reubi O, Blundy J (2009) A dearth of intermediate melts at subduction zone volcanoes and the petrogenesis of arc andesites. *Nature* 461:1269–1273
- Sethna SF (1999) Geology of Mumbai and surrounding areas and its position in the Deccan volcanic stratigraphy, India. *J Geol Soc India* 53:359–365
- Sethna SF, Battiwala HK (1974) Metasomatized basalt xenoliths in the trachyte of Manori-Goria, Bombay, and their significance. *Geological, Mining and Metallurgical Society of India Golden Jubilee Volume*: 337–346
- Sethna SF, Battiwala HK (1976) Hybridization effects in contemporaneous eruption of trachytic and basaltic magmas in Salsette Bombay. *Neues Jahrb Mineral* 11:495–507
- Sethna SF, Battiwala HK (1977) Chemical classification of the intermediate and acid rocks (Deccan Trap) of Salsette Island, Bombay. *J Geol Soc India* 18:323–330
- Sethna SF, Battiwala HK (1980) Major element geochemistry of the intermediate and acidic rocks associated with the Deccan Trap basalts. In: *Proceedings of the 3rd Indian Geological Congress*. Pune, pp 281–294
- Sethna SF, Battiwala HK (1984) Hybrid quartz-monzonite dyke near Dongri, Salsette island, Bombay. *The Indian Mineralogist*, pp 124–129
- Sheth HC, Melluso L (2008) The Mount Pavagadh volcanic suite, Deccan Traps: geochemical stratigraphy and magmatic evolution. *J Asian Earth Sci* 32:5–21
- Sheth HC, Ray JS (2002) Rb/Sr-⁸⁷Sr/⁸⁶Sr variations in Bombay trachytes and rhyolites (Deccan Traps): Rb-Sr isochron, or AFC process? *Int Geol Rev* 44:624–638
- Sheth HC, Pande K, Bhutani R (2001a) ⁴⁰Ar-³⁹Ar age of a national geological monument: the Gilbert Hill basalt, Deccan Traps, Bombay. *Curr Sci* 80:1437–1440
- Sheth HC, Pande K, Bhutani R (2001b) ⁴⁰Ar-³⁹Ar ages of Bombay trachytes: evidence for a Palaeocene phase of Deccan volcanism. *Geophys Res Lett* 28:3513–3516
- Sheth HC, Choudhary AK, Bhattacharyya S, Cucciniello C, Laishram R, Gurav T (2011) The Chogat–Chamardi subvolcanic complex, Saurashtra, northwestern Deccan Traps: geology, petrochemistry, and petrogenetic evolution. *J Asian Earth Sci*. doi:10.1016/j.jseaes.2011.02.012
- Snyder D (1997) The mixing and mingling of magmas. *Endeavour* 27:19–22
- Snyder D (2000) Thermal effects of the intrusion of basaltic magma into a more silicic magma chamber and implications for eruption triggering. *Earth Planet Sci Lett* 175:257–273
- Snyder D, Tait S (1998) The imprint of basalt on the geochemistry of silicic magmas. *Earth Planet Sci Lett* 160:433–445
- Sparks RSJ, Marshall LA (1986) Thermal and mechanical constraints on mixing between mafic and silicic magmas. *J Volc Geotherm Res* 29:99–124
- Straub SM, Gomez-Tuena A, Stuart FM, Zellmer GF, Cai Y, Espinasa-Perena R (2011) Formation of hybrid arc andesites beneath thick continental crust. *Earth Planet Sci Lett* 303:337–347
- Sun SS, McDonough WF (1989) Chemical and isotopic systematics of oceanic basalts: implications for mantle composition and processes. In: Saunders AD, Norry MJ (eds) *Magmatism in ocean basins*. Geological Society Special Publications, London, pp 313–345

- Thomas N, Tait SR (1997) The dimensions of magmatic inclusions as a constraint on the physical mechanism of mixing. *J Volc Geotherm Res* 75:167–178
- Verma SP, Torres-Alvarado IS, Sotelo-Rodriguez ZT (2002) SIN-CLAS: standard igneous norm and volcanic rock classification system. *Comput Geosci* 28:711–715
- Walker GPL, Skelhorn RR (1966) Some associations of acid and basic igneous rocks. *Earth Sci Rev* 2:93–109
- Yoder HS Jr (1973) Contemporaneous basaltic and rhyolitic magmas. *Am Mineral* 58:153–171
- Zellmer GF (2009) Petrogenesis of Sr-rich adakitic rocks at volcanic arcs: insights from global variations of eruptive style with plate convergence rates and surface heat flux. *J Geol Soc* 166:725–734
- Zellmer GF, Turner SP (2007) Arc dacite genesis pathways: evidence from mafic enclaves and their hosts in Aegean lavas. *Lithos* 95:346–362
- Zellmer GF, Sparks RSJ, Hawkesworth CJ, Wiedenbeck M (2003) Magma emplacement and remobilization timescales beneath Montserrat: insights from Sr and Ba zonation in plagioclase phenocrysts. *J Petrol* 44:1413–1431
- Zellmer GF, Rubin KH, Grönvold K, Jurado-Chichay Z (2008) On the recent bimodal magmatic processes and their rates in the Torfajökull–Veidivötn area, Iceland. *Earth Planet Sci Lett* 269:387–397